Bethe approximation for a system of hard rigid rods: the random locally tree-like layered lattice

Deepak Dhar
Department of Theoretical Physics, Tata Institute of Fundamental Research, Homi Bhabha Road, Mumbai 400005, India

R. Rajesh
The Institute of Mathematical Sciences, C.I.T. Campus, Taramani, Chennai 600113, India

Jürgen F. Stilck
Instituto de Física and National Institute of Science and Technology for Complex Systems, Universidade Federal Fluminense, Av. Litorânea s/n, 24210-346 Niterói, RJ, Brazil

(Dated: February 22, 2011)

We study the Bethe approximation for a system of long rigid rods of fixed length k, with only excluded volume interaction. For large enough k, this system undergoes an isotropic-nematic phase transition as a function of density of the rods. The Bethe lattice, which is conventionally used to derive the self-consistent equations in the Bethe approximation, is not suitable for studying the hard-rods system, as it does not allow a dense packing of rods. We define a new lattice, called the random locally tree-like layered lattice, which allows a dense packing of rods, and for which the approximation is exact. We find that for a 4-coordinated lattice, k-mers with $k \geq 4$ undergo a continuous phase transition. For even coordination number $q \geq 6$, the transition exists only for $k \geq k_{min}(q)$, and is first order.

PACS numbers: 64.70.mf,05.50.+q,64.60.Cn

I. INTRODUCTION

The study of the ordering transition in systems with only excluded volume interactions has a long history. Depending on the shape of the molecules involved, these systems can exhibit different ordered states and undergo transitions between them. Many different shapes have been studied in literature: e.g., hard spheres [1], hard squares [2, 3], hexagons [4], triangles [5], tetrominoes [6], rods [7], banana-shaped molecules [8], etc. A system of thin rigid cylindrical molecules in solution was shown by Onsager to undergo a first order phase transition from an isotropic to a nematic phase at sufficiently high densities, in the limit of large aspect ratio [9]. Flory studied the hard rods problem on a lattice [10], still allowing the rods to have continuous orientations, and using a mean-field approximation again found a isotropic-nematic transition. Zwanzig studied a system of hard rods in the continuum, but restricting their orientations to a discrete set [11], also finding a discontinuous transition to a nematic phase as the density of rods is increased. The relation between continuous and discrete models is discussed in Ref. [12].

For continuous models, in dimensions $d \geq 3$, if the aspect ratio of the rods is high enough, the existence of an isotropic–nematic transition is well accepted [7]. In two dimensions, in a system of hard needles in a plane, the Mermin–Wagner theorem [13] disallows long range orientational order, but at sufficiently high densities, the system shows a Kosterlitz-Thouless type ordering transition, and the orientational correlations decay with distance as a power law [14, 15]. If the rigid rods are placed on a lattice, then only a discrete set of orientations is possible, and the existence of a long-range ordered phase is not disallowed by the Mermin–Wagner theorem. Rods occupying k consecutive sites along any one lattice direction will be called k-mers. For dimers ($k = 2$), it can be shown rigorously that orientational correlations decay exponentially, except in the limit when all sites are occupied by rods. In the case of full coverage, the orientational correlations have a power law tail in all dimensions $d \geq 2$ [16, 17].

The question whether the lattice model of rigid rods with $k \gg 2$ undergoes a phase transition remained unsettled for a long time [18]. Clearly, the number of ways of covering the planar square lattice fully with k-mers grows exponentially with the size of the system, and most of these configurations are not ordered. Thus, at the maximum packing density, which was presumed to favour ordering most, the system shows no ordering. Recently, Ghosh and Dhar argued that k-mers on a square lattice, for $k \geq 7$, would undergo two phase transitions, and the nematic phase would exist for only an intermediate range of densities $\rho_1^* < \rho < \rho_2^*$, where $\rho_1^* \sim 1/k$ [19]. Subsequently, Fernandez et. al. [20–23], through extensive simulations and approximate methods, showed that the square lattice transition is Ising like, or equivalently in the liquid-gas universality class [24]. On the triangular and hexagonal lattices, there are three degenerate fully aligned ground states, and the transition was shown to be in the $q = 3$ Potts model universality class [20, 21]. The existence of a transition to a state with orientational order was shown rigorously for a polydispersed hard rod system on a two dimensional square lattice [25]. The second transition from nematic to unordered state at ρ_2^* is much less understood. In Ref. [19], a variational estimate

of the entropy of the nematic and ordered states suggests that $1-\rho_2^*$ should vary as $1/k^2$ for large k, but not much is known about the nature of transition. Linares et. al. estimated that $0.87 \leq \rho_2^* \leq 0.93$ for $k = 7$, and proposed an approximate functional form for the entropy as a function of the density [23].

Given the paucity of exact results about the second transition, it seems worthwhile to investigate this problem using well-known approximation methods, like the Bethe approximation (BA). However, we realized that there are problems in the application of the conventional BA techniques, even to the first isotropic–nematic transition. In particular, packing k-mers on the Bethe lattice with a density close to one seems difficult, and the nature of the high-density phase on the Bethe lattice is not very clear. Another way to study BA is to work with random graphs of fixed-coordination number [26–29]. In this case, there is no surface, but in this case as well, one does not get full coverage in the limit when the activity of k-mers tends to infinity. This has led us to introduce a new lattice, to be called the random locally tree-like layered lattice (RLTL lattice). We study k-mers on the RLTL and show that there is no difficulty in defining the high-density phase for the k-mers and that the BA is exact on this lattice. In fact, we find many ways to cover the lattice with k-mers. There is a finite entropy per site in the fully packed limit, and in a typical fully packed configuration, all k-mers are not all in the same orientation.

The rest of the paper is organised as follows. We begin with a recapitulation of the conventional approaches to the Bethe approximation, and the Bethe lattice in Sec. II, and derive self-consistent equations between different correlation functions. In Sec. III, we describe the RLTL lattice where every site in the lattice has the same even coordination number q. In Sec. IV, we derive the exact annealed partition function of the problem on this lattice, and show that the resulting self-consistent equations are the same as obtained earlier for the Bethe lattice. In Sec. V, we analyse the behaviour of these equations for the RLTL with coordination number 4, and show that it undergoes a continuous transition for $k > 4$. In Sec. VI, we discuss the case $q \geq 6$. We find that in this case, the system undergoes a first order transition for $k > k_{min}(q)$. Section VII contains some concluding remarks.

II. k-MERS ON A 4-COORDINATED BETHE LATTICE

The BA was initially proposed as an ad-hoc decoupling approximation (the pair approximation) [30, 31]. It was realized that the approximation becomes exact for the Bethe lattice, which is the part of a uniformly branching tree graph far away from the surface [32, 33]. This is important, as this ensures that the approximation can not give rise to unphysical consequences, like non-positive specific heat. Also, there is a consistent scheme, and two different answers for same quantity cannot be obtained. Given that in a uniformly branching tree, most of the sites are a finite distance from the surface, disentangling the surface contribution from that of sites deep inside requires some care [34–36]. There are some prescriptions for separating the surface contribution from bulk given in literature [37]. A rather careful and detailed discussion for the case of the Ising model on the Bethe lattice is given in Chapter 4 of Ref. [38]. One considers correlation functions deep inside a Cayley tree, whose values are independent of the boundary conditions on the surface of the tree. This can be realized for all non-zero external magnetic fields. Then thermodynamical quantities like the free energy are obtained by integrating these correlation functions with respect to suitable conjugate field.

A more recent approach to BA is to treat it as the free energy for a random graph on N sites, where each site in the graph has the same degree. One can show that in the limit N tends to infinity, for a randomly picked site in the graph, the length of the shortest loop increases as $\log N$. Then, the graph looks like a loop-less of uniform coordination number, up to a distance of order $\log N$. In the limit of large N, it looks like a Bethe lattice, except that there is no surface. This makes study of the different models on the Bethe lattice numerically feasible [26–29].

We first derive the self consistent equations satisfied by densities for the model of k-mers on a Bethe lattice of coordination number four in the conventional way. Generalisation to higher even coordination number is straightforward. A Bethe lattice corresponds to the core of the Cayley tree with the same coordination number. The sites of the Cayley tree may be ordered by its generation, starting with $m = 0$ for the sites on the surface and ending at $m = M$ for the central site of a tree with M generations. Each site of the Cayley tree, other than those on the surface, has 4 bonds attached to it. Two of them will be said to be of type X and the remaining two to be of type Y. A k-mer occupies $k-1$ consecutive bonds (and k sites) of the same type. We associate an activity z_1 with an X-type k-mer (referred to as X-mer in the following) and an activity z_2 with a Y-type k-mer (Y-mer). No two k-mers may overlap, so that each site of the lattice has at most one k-mer passing through it. Fig. 1 shows a four-coordinated Cayley tree occupied by three 4-mers.

The Cayley tree is composed of four rooted subtrees which are connected to the central site. We define partial partition functions for these rooted subtrees with fixed configuration of the root bond. We specify the type of the root bond and the configuration of the root bond. The root bond may be empty, or if it is occupied by a k-mer, then we specify the number of sites in earlier generations already occupied by this k-mer. There are $2k$ such partial partition functions, which we denote by $g_{x,j}$ and $g_{y,j}$, where the first subscript denotes the type of the root bond and $j = 1, \ldots, k-1$ is the number of sites that are currently part of the k-mer. $j = 0$ corresponds

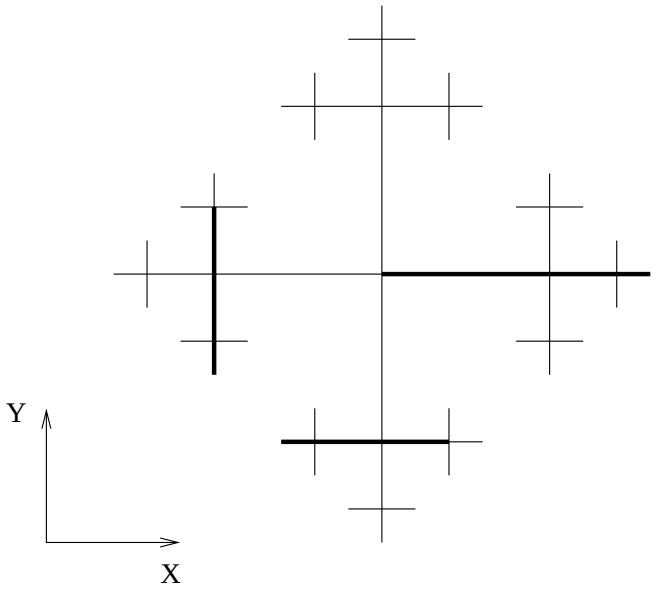

FIG. 1. A four-coordinated Cayley tree with four generations is shown. Two X-mers (horizontal thick solid lines) and one Y-mer (vertical thick solid line) with $k = 4$ are placed on the tree. The weight of the configuration is $z_1^2 z_2$.

to the case when the root bond is empty.

The recursion relations obeyed by the partial partition functions are obtained by building a subtree with one additional generation by connecting 3 subtrees to a new root bond and new root site. This process is illustrated in Fig. 2. We attach a weight $z_1^{1/k}$ and $z_2^{1/k}$ with each occupied site of and X-mer and Y-mer respectively. The recursion relations are (see Fig. 3)

$$g'_{x,0} = (g_{x,0} + z_1^{1/k} g_{x,k-1}) g_{y,0}^2 + z_2^{1/k} g_{x,0} \sum_{j=0}^{k-1} g_{y,j} g_{y,k-1-j}, \quad (1a)$$

$$g'_{y,0} = (g_{y,0} + z_2^{1/k} g_{y,k-1}) g_{x,0}^2 + z_1^{1/k} g_{y,0} \sum_{j=0}^{k-1} g_{x,j} g_{x,k-1-j}, \quad (1b)$$

$$g'_{x,j} = z_1^{1/k} g_{x,j-1} g_{y,0}^2, \quad j = 1, \ldots, k-1, \quad (1c)$$

$$g'_{y,j} = z_2^{1/k} g_{y,j-1} g_{x,0}^2, \quad j = 1, \ldots, k-1, \quad (1d)$$

where the prime denotes partial partition functions of subtrees with one additional generation of sites.

The partial partition functions are multiplied by the appropriate activity each time a k-mer grows such that the weight of a k-mer is z_1 or z_2 depending on its type. The partial partition functions grow exponentially with the number of iterations. To calculate the densities in the core of the tree (Bethe lattice), it is useful to define ratios of partial partition functions

$$R_{i,j} = \frac{g_{i,j}}{g_{i,0}}, \ i = x, y \text{ and } j = 0, \ldots, k-1, \quad (2)$$

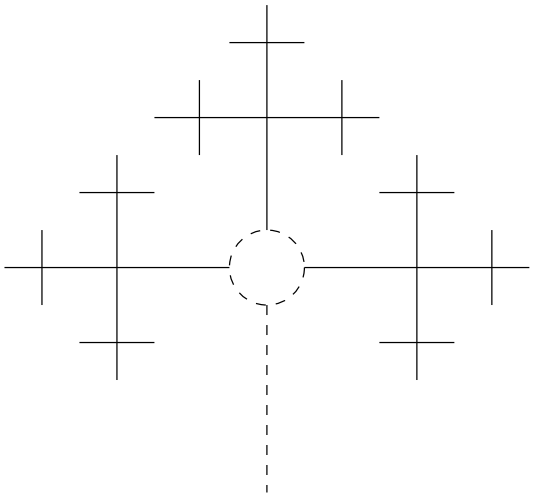

FIG. 2. Building a subtree with $M+1 = 4$ generations of sites by connecting $q - 1 = 3$ subtrees with $M = 3$ generations of sites to a new root site and bond (denoted by dashed lines). If the root bond of the new subtree is in the Y-direction, then two of the existing subtrees will have their root bond in the X-direction.

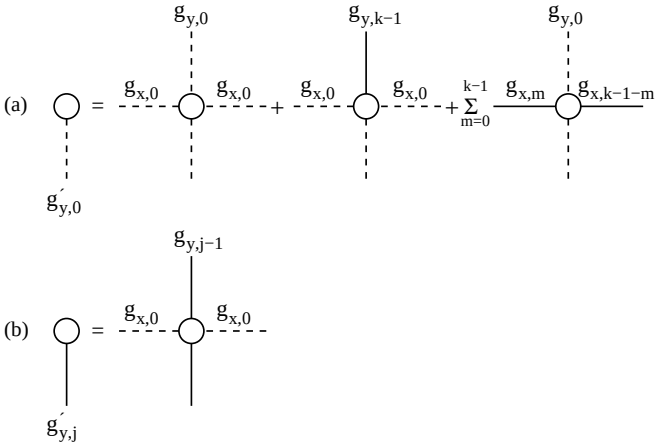

FIG. 3. Diagrammatic representation of Eq. (1) for $g'_{y,j}$, $j = 0, \ldots, k-1$.

such that $R_{x,0} = R_{y,0} = 1$. The recursion relations obeyed by the ratios are easily derived from Eq. (1):

$$R'_{x,j} = \frac{z_1^{1/k} R_{x,j-1}}{D_x}, \quad j = 1, \ldots, k-1, \quad (3a)$$

$$R'_{y,j} = \frac{z_2^{1/k} R_{y,j-1}}{D_y}, \quad j = 1, \ldots, k-1, \quad (3b)$$

where

$$D_x = 1 + z_1^{1/k} R_{x,k-1} + z_2^{1/k} \sum_{j=0}^{k-1} R_{y,j} R_{y,k-1-j}, \quad (4a)$$

$$D_y = 1 + z_2^{1/k} R_{y,k-1} + z_1^{1/k} \sum_{j=0}^{k-1} R_{x,j} R_{x,k-1-j}. \quad (4b)$$

We study the fixed points of these recursion relations. The fixed point corresponds to distance of the surface sites very large, or equivalently to sites in the deep interior of the Cayley tree. Also, if only one single stable fixed point exists, the boundary conditions at surface sites (which determine the initial values of the recursions), have no effect on the behaviour at points deep inside [35, 36].

A natural choice of the starting weights for the recursion equations are such that all k-mers are completely contained within the Cayley tree. This corresponds to $g_{x,0} = g_{y,0} = 1$, $g_{x,1} = z_1^{1/k}$, and $g_{y,1} = z_2^{1/k}$, with $g_{x,j} = g_{y,j} = 0$ for all $j > 1$. However, for these choices of initial conditions, the recursion relations under iteration converge to a fixed point that corresponds to the isotropic system because the initial conditions themselves are symmetric. The isotropic fixed point is stable with respect to perturbations where the initial conditions are still symmetric with respect to the two directions. However, it is unstable to asymmetric perturbations.

For generic initial conditions, we find that on repeatedly iterating the recursion relations, the R's converge to a stable fixed point R^*, which may be determined by iterating Eq. (3). Then,

$$R^*_{x,j} = \left(\frac{z_1^{1/k}}{D_x}\right)^j \equiv \alpha_x^j,\ j = 0, \ldots, k-1, \tag{5a}$$

$$R^*_{y,j} = \left(\frac{z_2^{1/k}}{D_y}\right)^j \equiv \alpha_y^j,\ j = 0, \ldots, k-1, \tag{5b}$$

where the variables α_x, α_y satisfy the equations

$$\alpha_x[1 + z_1^{1/k}\alpha_x^{k-1} + kz_2^{1/k}\alpha_y^{k-1}] = z_1^{1/k}, \tag{6a}$$

$$\alpha_y[1 + z_2^{1/k}\alpha_y^{k-1} + kz_1^{1/k}\alpha_x^{k-1}] = z_2^{1/k}. \tag{6b}$$

Knowing the fixed point solution, the density at the central site may be calculated. The grand canonical partition function of the system on the Cayley tree is given by

$$\Xi = g_{x,0}^2 g_{y,0}^2 + z_1^{1/k} g_{y,0}^2 \sum_{j=0}^{k-1} g_{x,j} g_{x,k-1-j} + z_2^{1/k} g_{x,0}^2 \sum_{j=0}^{k-1} g_{y,j} g_{y,k-1-j}. \tag{7}$$

Then, the densities ρ_x (ρ_y) of sites that are part of X-mers (Y-mers) are given by

$$\rho_x = \frac{z_1^{1/k} g_{y,0}^2 \sum_{j=0}^{k-1} g_{x,j} g_{x,k-1-j}}{\Xi}, \tag{8a}$$

$$\rho_y = \frac{z_2^{1/k} g_{x,0}^2 \sum_{j=0}^{k-1} g_{y,j} g_{y,k-1-j}}{\Xi}, \tag{8b}$$

At the fixed points, the densities simplify to

$$\rho_x = \frac{k z_1^{1/k} \alpha_x^{k-1}}{1 + k z_1^{1/k} \alpha_x^{k-1} + k z_2^{1/k} \alpha_y^{k-1}}, \tag{9a}$$

$$\rho_y = \frac{k z_2^{1/k} \alpha_y^{k-1}}{1 + k z_1^{1/k} \alpha_x^{k-1} + k z_2^{1/k} \alpha_y^{k-1}}. \tag{9b}$$

Eliminating α_x, α_y from Eqs. (9) and Eqs. (6), we obtain

$$z_1(1 - \rho_x - \rho_y)^k = \frac{\rho_x}{k}\left(1 - \frac{k-1}{k}\rho_x\right)^{k-1}, \tag{10a}$$

$$z_2(1 - \rho_x - \rho_y)^k = \frac{\rho_y}{k}\left(1 - \frac{k-1}{k}\rho_y\right)^{k-1}. \tag{10b}$$

The Bethe lattice solution described above is not very satisfactory. In particular, in the limit of large z_1 and z_2, one gets the fraction of sites occupied by k-mers tends to 1. However, it is easy to see that this can only be achieved with a very special choice of boundary conditions at the surface of the tree.

Also, if we consider a tree with coordination number $q \geq 6$, in the large activity limit, then at any root vertex of a subtree, the process of exchanging different branches is clearly a symmetry operation on the lattice. It is easy to see that the presence of this local symmetry implies that there can be no nematic order in the deep inside region, with one type of bonds preferentially occupied. This makes this approach unsuitable for the studies of the hard rod problem.

III. THE RLTL LATTICE CONSTRUCTION

For simplicity, we discuss the random lattice with coordination number $q = 4$. Generalisation to other coordination numbers is straight forward. We consider a set of M layers, numbered from 1 to M, with N sites in each layer. A layer m is connected to the adjacent layer $m-1$ by N bonds of type X and N bonds of type Y. The connections are made by randomly pairing each site of the mth layers with exactly one site in the $(m-1)$-th layer with an X-bond, similarly randomly pairing each site with a site in the neighbouring layer using Y-bonds. The total number of such possible pairings is $(N!)^2$. This is illustrated in Fig. 4.

We can impose open or periodic boundary conditions. For a $2q$ coordinated lattice, there are $(N!)^{qM}$ different possible graphs, in the case of periodic boundary conditions (layer M is connected to layer 1), and $(N!)^{q(M-1)}$ different possible graphs for the case of open boundary conditions. We consider annealed models on this lattice, thus we average the partition function over all possible configurations of the bonds.

We can associate different degrees of freedom with the vertices, and consider statistical mechanical models on these lattices. For example, we can attach an Ising spin

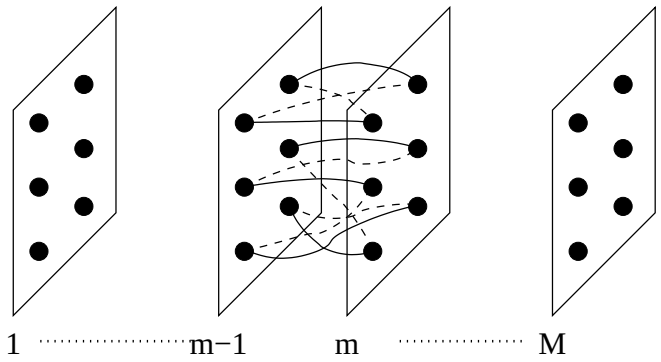

FIG. 4. Schematic diagram of the random lattice with $N = 6$ sites per layer and coordination number $q = 4$. A possible configuration of bonds between layers $m-1$ and m is shown, with the solid and dotted lines being bonds of two different types.

S_j to each vertex j of the lattice, and define the Hamiltonian to be $H = -J\sum_{nn} S_i S_j$, where the sum is over all nearest neighbour pairs. For a particular realization $\mathcal{R}$ of bonds, let the partition function be $\mathcal{Z}_{\mathcal{R}}(M,N)$. We average the partition function over all possible configurations of bonds. As we are averaging the partition function, and not the logarithm of the partition function, this is similar to the annealed average over different bond configurations. Thus,

$$Z_{av}(M,N) = \frac{1}{N_{\mathcal{R}}}\sum_{\mathcal{R}} \mathcal{Z}_{\mathcal{R}}(M,N), \tag{11}$$

where $N_{\mathcal{R}}$ is the number of different bond configurations on the lattice.

To take the thermodynamic limit, we let M and N tend to infinity. The mean free energy per site f is defined as the limit

$$f = -kT \lim_{M,N\to\infty} \frac{1}{MN}\log Z_{av}(M,N). \tag{12}$$

We note that each site, say in layer m, has exactly one X-bond, and one Y-bond connecting it to sites in the layer $m+1$. It can happen that these bonds fall on the same site. However, the fractional number of such cases is only $1/N$, and thus, the expected number of loops of size 2 on this lattice is M. For M even, the graph is bipartite, and there are no loops of odd perimeter. It is easy to verify that the expected number of loops of perimeter 4 on this lattice is $5M$. In general, the number of loops of perimeter ℓ per site of the lattice varies as λ^{ℓ}/N, where λ is the self-avoiding walk growth constant [39].

We, thus, see that for large N, there are very few short loops in the lattice. For a randomly picked site, the size of the shortest loop going through that site is of order $\log N$, and this goes to infinity, as N goes to infinity. Since there are very few short loops, the structure of the lattice locally is that of a regular branching tree, and it locally looks like the Bethe lattice.

The correlation functions can be defined as usual. Consider the example of the Ising model defined above. We consider two sites i and j, and consider the two-point correlation function $\langle S_i S_j\rangle$. Since this correlation function has to be averaged over all assignments of bonds, it can depend only on the difference in layer numbers of the sites. In particular, it has the same value for all sites i and j in the same layer. Thus, the expected factorisation property of the correlation functions, which is the essence of the Bethe approximation, is built into the definition of the lattice.

IV. k-MERS ON THE RLTL LATTICE WITH $q = 4$

We consider a k-mer model on the RLTL lattice. A k-mer occupies $(k-1)$ consecutive bonds of the same type. As earlier, we associate an activity z_1 with an X-mer and an activity z_2 with a Y-mer.

Let x_m be the number of X-mers with topmost (1^{st}) site in the m-th layer, and y_m is number of Y-mers with topmost site in the m-th layer. We will denote by X_m and Y_m, the number of sites in the mth layer, occupied by X-type, and Y-type bonds respectively, but where the site is not the topmost site of the k-mer. Clearly, we have

$$X_m = \sum_{j=1}^{k-1} x_{m-j}, \quad Y_m = \sum_{j=1}^{k-1} y_{m-j}. \tag{13}$$

We can adopt the convention that $x_m = y_m = 0$, for $m \le 0$. Then the above equation holds for all $m, 1 \le m \le M$. Note that if we want the k-mers to be fully contained in the lattice, we must also have $x_m = y_m = 0$, for $m \ge M - k + 2$.

To calculate the partition function, consider the operation of adding an additional layer. We, thus, specify the full set of $2M$ values $\{x_m, y_m\}$ for all m. The total statistical weight of configurations that contribute to a particular set $\{x_m, y_m\}$ will be denoted by $C(\{x_m, y_m\})$.

We calculate $C(\{x_m, y_m\})$ recursively. Let us imagine that we have constructed the configuration of the lattice to layer $m-1$, and now we add the layer m. We sum over the configurations of bonds, and that of X-mers and Y-mers on these bonds at the same time.

(i) We note that in the $(m-1)$-th layer, there are X_m sites that are occupied by X-mers which protrude to layer m. The first of these sites is connected to a randomly picked site in the lower layer in N ways using an X-bond. Then this site in the lower layer is occupied by the extension of that X-mer. The next can be connected to one of the unoccupied sites in the lower layers in only $(N-1)$ ways. Similarly the third, and so on. The number of ways to do this is:

$$\frac{N!}{(N-X_m)!}.$$

(ii) Now we take the Y_m Y-mers in the $(m-1)$-th layer that are extending down to the lower layer. Number of ways of extending these to the $(N-X_m)$ unoccupied sites below is clearly

$$\frac{(N-X_m)!}{(N-X_m-Y_m)!}.$$

(iii) Connect the remaining $N-X_m$ X-bonds between layers $m-1$ and m to sites in layer m not yet connected by X bonds. The number of ways to do this is

$$(N-X_m)!.$$

(iv) Repeat the last procedure with the $N-Y_m$ remaining Y-bonds between the layers m and $m+1$. The number of ways to do this is

$$(N-Y_m)!.$$

(v) Finally, the $(N-X_m-Y_m)$ sites in layer m, that are unoccupied so far, are divided into three groups: x_m topmost sites of new X-mers, y_m topmost sites of new Y-mers, and the unoccupied sites. Clearly the number of ways to do this is:

$$\frac{(N-X_m-Y_m)!}{x_m!y_m!(N-X_m-Y_m-x_m-y_m)!}.$$

The product of these factors gives the total number of ways of adding the m-th layer as:

$$\frac{N!(N-X_m)!(N-Y_m)!}{x_m!y_m!(N-X_m-Y_m-x_m-y_m)!}. \tag{14}$$

Finally, multiplying these factors for different m, we get the configurations with specified $\{x_m, y_m\}$ have total number of configurations $C(\{x_m, y_m\})$ given by

$$C(\{x_m,y_m\}) = \prod_{m=1}^{M} \frac{N!(N-X_m)!(N-Y_m)!}{x_m!y_m!(N-X_m-Y_m-x_m-y_m)!}. \tag{15}$$

Putting in the corresponding activity factors, the grand partition function for the whole lattice with M layers is

$$Z_{av} = \frac{1}{(N!)^{2M-2}} \sum_{\{x_m,y_m\}} C(\{x_m,y_m\}) z_1^{\sum x_m} z_2^{\sum y_m}, \tag{16}$$

where the sum is over all possible values of $\{x_m, y_m\}$), and we have divided the multiplicity factor by the number of configurations of the random lattice $(N!)^{2M-2}$, to get the average partition function. Note that $Z_{av} = 1$ for $z_1 = z_2 = 0$, as expected.

The summation over $\{x_m, y_m\}$ yields at most a factor of order N^{2M}. Since the summand is of order $\exp(NM)$, for large N, we can ignore the summation over $\{x_m, y_m\}$, and replace the summation with the largest term, with negligible error. For the summand to be maximum with respect to x_j, we set

$$\frac{C(\{x_m+\delta_{m,j}, y_m\})z_1}{C(\{x_m,y_m\})} \approx 1. \tag{17}$$

This gives

$$z_1 \prod_{s=0}^{k-1} \frac{(N-X_{j+s}-x_{j+s}-Y_{j+s}-y_{j+s})}{(N-X_{j+s})} = \frac{x_j+1}{(N-X_j)}, \tag{18}$$

and similarly

$$z_2 \prod_{s=0}^{k-1} \frac{(N-X_{j+s}-x_{j+s}-Y_{j+s}-y_{j+s})}{(N-Y_{j+s})} = \frac{(y_j+1)}{(N-Y_j)}. \tag{19}$$

Writing the maximising values as $f_j^* = x_j/N$ and $g_j^* = y_j/N$, the equations satisfied by f_j^* and g_j^* in the limit N tends to infinity are

$$z_1 \prod_{s=0}^{k-1} \frac{1-\rho_x(j+s)-\rho_y(j+s)}{1-\rho_x(j+s)+f_{j+s}^*} = \frac{f_j^*}{1-\rho_x(j)+f_j^*} \tag{20}$$

$$z_2 \prod_{s=0}^{k-1} \frac{1-\rho_x(j+s)-\rho_y(j+s)}{1-\rho_y(j+s)+g_{j+s}^*} = \frac{g_j^*}{1-\rho_y(j)+g_j^*} \tag{21}$$

where $\rho_x(m)$ and $\rho_y(m)$ are the fractions of sites in layer m covered by X-mers and Y-mers respectively. Clearly,

$$\rho_x(j) = \sum_{s=0}^{k-1} f_{j-s}^*, \quad \rho_y(j) = \sum_{s=0}^{k-1} g_{j-s}^*. \tag{22}$$

These equations connect f_j^* and g_j^* to their value of f_{j+s}^* and g_{j+s}^*, with $s = 1$ to $k-1$. These may be considered as recursion equations for f_j^*, g_j^*. These recursions work in the direction of decreasing j.

These equations have a simple interpretation. In the equilibrium state, z_1 is the ratio of the probability that a randomly chosen site will be the head of a X-mer to the probability that an X-mer can be placed with this site as the head. The probability that the chosen site is empty is $[1-\rho_x(j)-\rho_y(j)]$. Given that a given site is empty in layer $(j'-1)$, the conditional probability that the site connected to it in the layer j' by an X-bond is also empty is $\frac{1-\rho_x(j')-\rho_y(j')}{1-\rho_x(j')+f_{j'}^*}$. Multiplying these probabilities for $(k-1)$ consecutive layers, we get the probability that a given site in layer j can be the head of an X-mer to be

$$\frac{\prod_{s=0}^{k-1}[1-\rho_x(j+s)-\rho_y(j+s)]}{\prod_{s=1}^{k-1}[1-\rho_x(j+s)+f_{j+s}^*)]}.$$

The probability that the chosen site in the jth layer is the head of an X-mer is f_j^*. The ratio of these is $1/z_1$, which gives Eq. (18).

The simplest solution of this is a fixed point solution with $f_j^* = f^*$, $g_j^* = g^*$, independent of j (away from the boundaries). Then f^*, g^* satisfy the equations

$$z_1(1-kf^*-kg^*)^k = f^*[1-(k-1)f^*]^{k-1}, \tag{23a}$$

$$z_2(1-kf^*-kg^*)^k = g^*[1-(k-1)g^*]^{k-1}. \tag{23b}$$

These equations are the same as Eq. (10), and we have recovered the Bethe approximation. However, for the RLTL lattice, the limit of fully packed lattice is well-defined, and causes no difficulties.

From Eq. (15), the entropy per site (divided by k_B) is easily seen to be

$$\begin{aligned} s(\rho_x,\rho_y) = &\left(1-\frac{k-1}{k}\rho_x\right)\ln\left(1-\frac{k-1}{k}\rho_x\right) \\ &+\left(1-\frac{k-1}{k}\rho_y\right)\ln\left(1-\frac{k-1}{k}\rho_y\right) \\ &-(1-\rho)\ln(1-\rho)-\frac{\rho_x}{k}\ln\frac{\rho_x}{k}-\frac{\rho_y}{k}\ln\frac{\rho_y}{k}, \end{aligned} \tag{24}$$

where $\rho = \rho_x + \rho_y$ is the total density. The same expression for entropy was obtained by DiMarzio [21, 40] who used an approximate counting technique for counting configurations on cubic lattices in any dimension. Also, Eq. (24) coincides with the expression for entropy that one obtains by using Gujrati's prescription for calculating free energies on the Bethe lattice [37].

It is easy to see that this expression for the entropy is not everywhere convex. When the value of $s(\rho_x,\rho_y)$, calculated as above, turns out to be in the non-convex region, it is easily seen that a much larger contribution to the partition function comes from $\{x_m, y_m\}$ that are not nearly uniform, and in a canonical ensemble at fixed ρ_x and ρ_y, the lattice will show phase separation, with one region having higher density than the other. The net effect of this to replace non-convex parts of the entropy function by a convex envelope construction. Thus, we write the true entropy $\tilde{s}(\rho_x,\rho_y)$ as

$$\tilde{s}(\rho_x,\rho_y) = \mathcal{CE}\left[s(\rho_x,\rho_y)\right], \tag{25}$$

where $\mathcal{CE}$ denotes convex envelope.

V. ISOTROPIC–NEMATIC TRANSITION

In this section, we analyse the isotropic–nematic transition when the coordination number is four. From Eq. (24), the expression for entropy, it is straight forward to determine the ordering that has maximum entropy.

Consider the system at a fixed density $\rho = \rho_x + \rho_y$. We define the order parameter ψ by

$$\psi = \frac{\rho_x - \rho_y}{\rho}. \tag{26}$$

Then, it is easy to study the variation of $s(\rho_x,\rho_y)$ as a function of ψ, for fixed ρ. We find that for small ρ, the entropy has a single maximum at $\psi = 0$, but for large enough $\rho > \rho_c$, it develops two symmetrically placed maxima (see Fig. 5). For small ψ, we can expand the entropy in a power series around $\psi = 0$ as in the standard Landau treatment

$$s(\rho_x,\rho_y) = A(\rho) - \psi^2 B(\rho) + \psi^4 C(\rho) + \ldots. \tag{27}$$

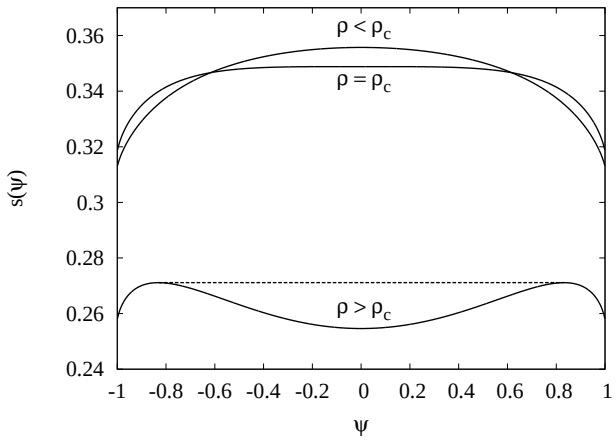

FIG. 5. Entropy as a as a function of the order parameter ψ for different densities. The data are for $q = 4$, $k = 4$ when the transition is continuous. Entropy has one peak for small densities and two symmetric peaks for large densities. The dotted lines denotes the convex envelope.

The coefficient of the quadratic term $B(\rho)$ changes sign at $\rho = \rho_c$, and is negative for larger ρ. Thus, for $\rho > \rho_c$, we have a nematic phase, with nonzero value of ψ. The critical exponent for β for the order parameter takes the classical Landau theory value 1/2.

The value of ρ_c can be determined easily from Eq. (23). For $z_1 = z_2 = z$, we note that both f^* and g^* are solutions to an equation of the form

$$x\left(1-\frac{k-1}{k}x\right)^{k-1} = constant. \tag{28}$$

The left hand side of the equation is a function of x that starts at 0 for $x = 0$, increases to a maximum value, and then decreases monotonically, and reaches a positive finite value $(1/k)^{k-1}$, for $x = 1$. When the right hand constant is small enough, there is only one real valued solution of this equation, and $f^* = g^*$. For a range of values of the constant, there are exactly two distinct solutions. At the critical point, the two solutions are degenerate. This occurs where the function is maximum, i.e., at

$$x^* = \frac{1}{k-1}. \tag{29}$$

Then at this point $f^* = g^* = x^*/k$, and $\rho_x = \rho_y = 1/(k-1)$. Correspondingly, we have $\rho_c = 2/(k-1)$. The corresponding value of critical activity, from Eq. (23), is

$$z_c = \frac{(k-1)^{2k-2}}{[k(k-3)]^k}, \quad q = 4. \tag{30}$$

We note that the value of z_c is finite only for $k \geq 4$. In Fig. 6, we show the variation of the modulus of the order parameter $|\psi|$ with density ρ for different rod lengths k. $|\psi|$ is non–zero for densities larger than the critical density.

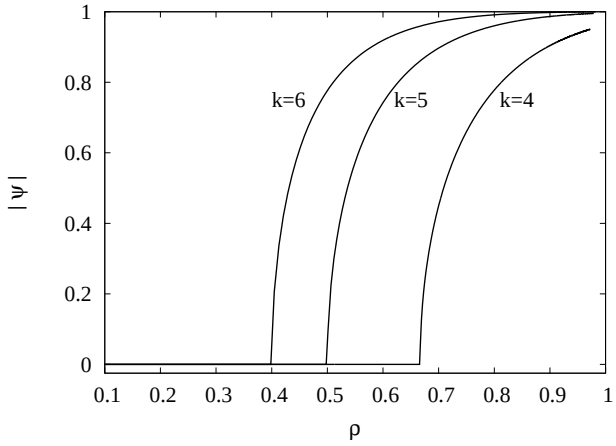

FIG. 6. The modulus of nematic order parameter ψ as a function of the density ρ for different rod lengths k. The data are for $q = 4$.

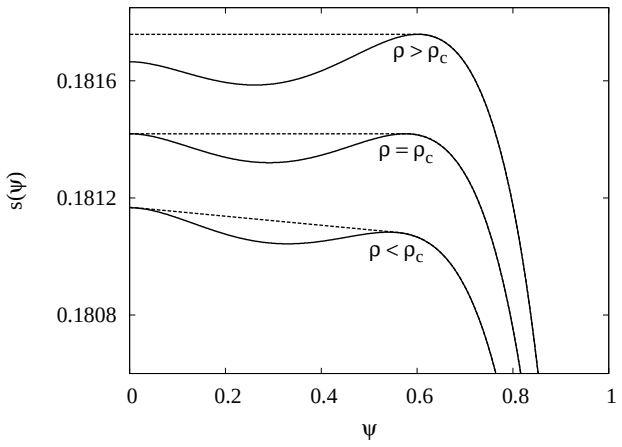

FIG. 7. Entropy as a as a function of the order parameter ψ for different densities. The data are for $q = 6$, $k = 8$, when the isotropic–nematic transition is first order. The different curves correspond to (a) $\rho = 0.3890$, (b) $\rho = 0.3910 \approx \rho_c$, (c) $\rho = 0.3930$. The dotted line shows the convex envelope.

VI. LATTICES WITH COORDINATION NUMBER $q \geq 6$

The analysis of $q \geq 6$ is very similar. It is easy to check that for general even q, the fixed point solution which is independent of the layer index j, satisfies the self-consistent equations

$$kz(1-\rho)^k = \rho_i \left[1 - \frac{k-1}{k}\rho_i\right]^{k-1}, \; i = 1, \ldots, \frac{q}{2}, \quad (31)$$

where i labels the $q/2$ different bond types, and $\rho = \sum_i \rho_i$ is the total density of sites that are part of k-mers. The entropy per site generalises to

$$s = \sum_{i=1}^{q/2} \left(1 - \frac{k-1}{k}\rho_i\right) \ln\left(1 - \frac{k-1}{k}\rho_i\right) - (1-\rho)\ln(1-\rho) - \sum_{i=1}^{q/2} \frac{\rho_i}{k} \ln \frac{\rho_i}{k}. \quad (32)$$

The low density phase is isotropic, with ρ_i same for different i. We define the order parameter to be $\psi = (\rho_1 - \rho_2)/\rho$, with $\rho_2 = \ldots = \rho_{q/2}$. But now the entropy function has no symmetry under $\psi \to -\psi$. Then, the expansion of $s(\rho_i)$ in powers of ψ contains cubic terms. Fig. 7 shows the behaviour of entropy as a function of ψ for different densities ρ when $q = 6$. For small ρ, there is a single maximum at ψ equal to zero. For larger ρ, a second local maximum at a non-zero ψ appears, and at some value of ρ this becomes of equal height. Then the order parameter jumps discontinuously, as the density is increased.

In Fig. 8, we show the variation of the order parameter ψ with density ρ for $q = 6$ and different values of k, and for $k = 5$ and different values of q. The first order transition is clearly seen, with the critical activity increasing with q and decreasing with k.

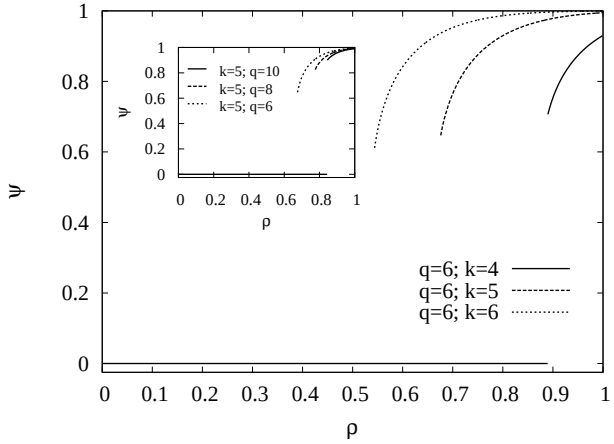

FIG. 8. The order parameter as a function of density ρ for $q = 6$ and varying k. There is a first order transition at a critical value ρ_c which decreases with k. Inset: The order parameter ψ as a function of ρ for $k = 5$ and varying q. ρ_c increases with q.

For coordination number greater than four, it is not possible to determine the critical density exactly. The critical densities obtained by numerically comparing the entropy of the isotropic and nematic phases are summarised in Fig. 9. For a fixed value of q, $\rho_c \sim \ln(q)/k$ for large k.

As expected in discontinuous transitions, in a range of values for the densities around the critical density ρ_c, entropy has a local maximum for both the isotropic ($\psi = 0$) and nematic phases. In Fig. 10, the values of densities at which these local maxima appear and disappear, along with the critical density are shown for $k = 5$ and $k = 8$ for different values of q. Only for $q = 4$, where the transitions are continuous, all the densities coincide.

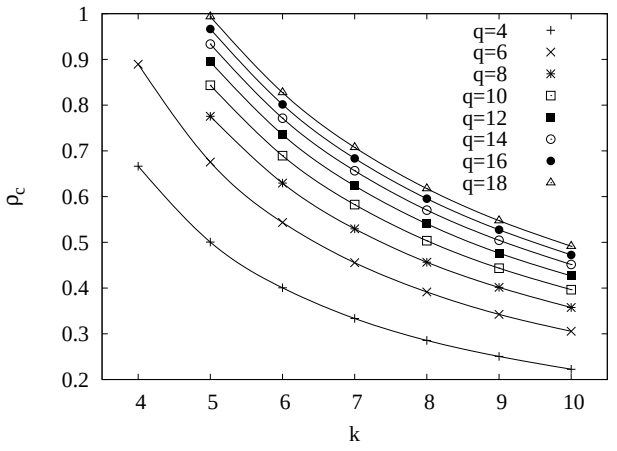

FIG. 9. The critical density ρ_c of the isotropic–nematic phase transition as a function of k for different values of the coordination number q. For $q = 4$ the transition is continuous.

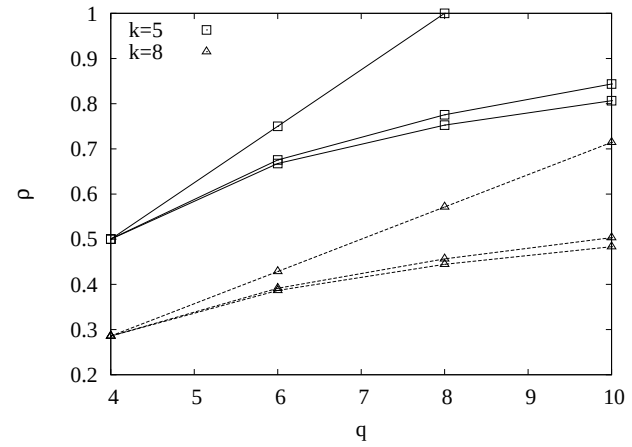

FIG. 10. Coexistence and limits of stability values of density of the isotropic and nematic phases as functions of q for two different rod lengths. For given values of q and k, the lowest point is the is the density at which $s(\psi)$ develops a second local maximum, the intermediate point is the critical density ρ_c, and the highest point is the density at which $s(\psi)$ is no longer a local maximum at $\psi = 0$. The lines are guides to the eye.

It is possible to determine the spinodal density ρ_s, the density at which the entropy $s(\psi)$ no longer has a maximum at $\psi = 0$. As in the analysis of $q = 4$, the spinodal is still given by the condition $x^* = 1/(k-1)$. But now that there are $q/2$ distinct directions, the density at the spinodal point is $q/[2(k-1)]$. If $q < 2(k-1)$, the spinodal density is less than one, and entropy will have a maximum at the nematic fixed point. Thus, there is always a phase transition for $q < 2(k-1)$.

We now address the question of whether for coordination number q, there is a minimum rod length k_{min} below which the isotropic–nematic transition is absent. From the analysis of the spinodal,

$$k_{min} \leq \frac{q+4}{2}. \tag{33}$$

The precise value of k_{min} is computed numerically and the results are shown in Table I. We find that $k_{min} \sim \ln(q)$.

TABLE I. The minimum rod length k_{min} required for an isotropic–nematic transition as a function of coordination number q.

q	k_{min}	q	k_{min}
$q \in [4, 6]$	4	$q \in [656, 1612]$	10
$q \in [8, 18]$	5	$q \in [1614, 3994]$	11
$q \in [20, 44]$	6	$q \in [3996, 9968]$	12
$q \in [46, 110]$	7	$q \in [9970, 25028]$	13
$q \in [112, 266]$	8	$q \in [25030, 63188]$	14
$q \in [268, 654]$	9		

VII. DISCUSSION

We are not able to address the nature of the second transition in this study, as on the RLTL lattice, there is none. However, on this lattice, the limit of fully packed lattice is quite interesting. We find that in this limit, the system has long-range nematic order, but the ordering is not complete, and there are small islands of "wrongly" oriented k-mers in a sea of aligned k-mers. The small concentration of these wrongly oriented rods is entropically stabilised.

The order parameter ψ is easy to determine for $k = 4$, when

$$\psi = \begin{cases} \frac{5\sqrt{3}}{9} \approx 0.96225, & \text{k=4, q=4,} \\ \frac{3(\sqrt{6}-4)}{5} \approx 0.93031, & \text{k=4, q=6,} \\ \frac{13}{15} \approx 0.86667, & \text{k=4, q=8.} \end{cases} \tag{34}$$

The limiting value of ψ grows monotonically with k, being equal to 1 in the limit $k \to \infty$. It is easy to see that the nematic order parameter has the asymptotic behaviour

$$1 - \psi \approx \frac{q}{2k^{k-1}}, \quad k \to \infty. \tag{35}$$

We can also look for a periodic solution of period k, where $x_{m+k} = x_m, y_{m+k} = y_m$. In this case, the $2k$ independent parameters f_s^*, g_s^*, with $s = 0$ to $k-1$ satisfy the equations

$$f_j^*(1 - \rho_1 + f_j^*) = z_1(1 - \rho_1 - \rho_2)^k/A, \tag{36}$$
$$g_j^*(1 - \rho_2 + g_j^*) = z_2(1 - \rho_1 - \rho_2)^k/B,$$

where

$$\rho_1 = \sum_{s=0}^{k-1} f_s^*; \rho_2 = \sum_{s=0}^{k-1} g_s^*, \tag{37}$$

and

$$A = \prod_{s=0}^{k-1} [1 - \rho_1 + f_s^*] \, ; B = \prod_{s=0}^{k-1} [1 - \rho_y + g_s^*] \, . \qquad (38)$$

In Eq. (37), the left hand side is a function of the form $(x + cx^2)$, with c positive, and the right hand side is independent of j. Hence, the only positive real solution of this equation is of the form f_j^* independent of j, and we do not get a non-trivial periodic solution. Note that a periodic solution would correspond to smectic-like layered ordering, and our solution rules it out.

We can easily extend our treatment to semi-flexible rods, where all the rods are aligned in the direction of increasing layer number, but a k-mer lying on an X-bond between layers j and $(j = 1)$ can bend, and lie on a Y-bond between layers $(j+1)$ and $(j+2)$, with some energy cost. Solutions for flexible and semi-flexible polymers on Bethe and Husimi lattices can be found in Refs. [41, 42].

There are other models like the ANNNI model [43], where exact solution in dimensions greater than one is not possible, and the equilibrium state shows spatial structure. These are usually discussed in the spatially varying mean-field approximation. We feel that studying such model on RLTL lattice can take into account the short-range correlations in these systems better.

ACKNOWLEDGMENTS

The work of DD and RR was partially supported by the Department of Science and Technology, Government of India under the project DST/INT/Brazil/RPO-40/2007, and that of JFS by CNPq under the project 490843/2007-7. We thank Ronald Dickman for a careful reading of the manuscript.

[1] N. Clisby and B. M. McCoy, Pramana **64**, 775 (2005).
[2] P. A. Pearce and K. A. Seaton, J. Stat. Phys. **53**, 1061 (1988).
[3] H. C. M. Fernandes, J. J. Arenzon, and Y. Levin, J. Chem. Phys. **126**, 114508 (2007).
[4] R. J. Baxter, J. Phys. A: Math. Gen. **13**, L61 (1980).
[5] A. Verberkmoes and B. Nienhuis, Phys. Rev. Lett. **83**, 3986 (1999).
[6] B. C. Barnes, D. W. Siderius, and L. D. Gelb, Langmuir **25**, 6702 (2009).
[7] G. J. Vroege and H. N. W. Lekkerkerker, Rep. Prog. Phys. **55**, 1241 (1992).
[8] Y. Maeda, T. Niori, J. Yamamato, and H. Yokoyoma, Thermochimica Acta **431**, 87 (2005).
[9] L. Onsager, Ann. N.Y. Acad. Sci. **51**, 627 (1949).
[10] P. J. Flory, Proc. R. Soc. **234**, 60 (1956).
[11] R. Zwanzig, J. Chem. Phys. **39**, 1714 (1963).
[12] K. Shundyak and R. Roij, Phys. Rev. E **69**, 041703 (2004).
[13] N. D. Mermin and H. Wagner, Phys. Rev. Lett. **17**, 1133 (1966).
[14] D. Frenkel and R. Eppenga, Phys. Rev. A **31**, 1776 (1985).
[15] M. D. Khandkar and M. Barma, Phys. Rev. E **72**, 051717 (2005).
[16] O. J. Heilmann and E. Lieb, Commun. Math. Phys. **25**, 190 (1972).
[17] D. A. Huse, W. Krauth, R. Moessner, and S. L. Sondhi, Phys. Rev. Lett. **91**, 167004 (2003).
[18] P. G. de Gennes and J. Prost, *The Physics of Liquid Crystals* (Oxford University Press, Oxford, 1993).
[19] A. Ghosh and D. Dhar, Euro. Phys. Lett. **78**, 20003 (2007).
[20] D. A. Matoz-Fernandez, D. H. Linares, and A. J. Ramirez-Pastor, Euro. Phys. Lett **82**, 50007 (2008).
[21] D. A. Matoz-Fernandez, D. H. Linares, and A. J. Ramirez-Pastor, Physica A **387**, 6513 (2008).
[22] D. A. Matoz-Fernandez, D. H. Linares, and A. J. Ramirez-Pastor, J. Chem. Phys. **128**, 214902 (2008).
[23] D. H. Linares, F. Romá, and A. J. Ramirez-Pastor, J. Stat. Mech., P03013(2008).
[24] T. Fischer and R. L. C. . Vink, Euro. Phys. Lett. **85**, 56003 (2009).
[25] D. Ioffe, Y. Velenik, and M. Zahradnik, J. Stat. Phys. **122**, 761 (2006).
[26] C. Baillie, D. A. Johnston, and J. P. Kownacki, Nucl. Phys. B **432**, 551 (1994).
[27] D. Dhar, P. Shukla, and J. P. Sethna, J. Phys. A **30**, 5259 (1997).
[28] A. Dembo and A. Montanari, Annals of Appl. Prob. **20**, 565 (2010).
[29] A. Dembo and A. Montanari, Brazilian J. of Prob. and Stat. **24**, 137 (2010).
[30] H. A. Bethe, Proc. Roy. Soc. A **150**, 552 (1935).
[31] G. S. Rushbrooke, Proc. Roy. Soc. A **166**, 296 (1938).
[32] M. Kurata, R. Kikuchi, and T. Watari, J. Chem. Phys. **21**, 434 (1953).
[33] G. S. Rushbrooke and H. I. Scoins, Proc. Roy. Soc. A **230**, 74 (1955).
[34] L. K. Runnels, J. Math. Phys. **8**, 2081 (1967).
[35] T. P. Eggarter, Phys. Rev. B **9**, 2989 (1973).
[36] E. Müller-Hartmann and J. Zittartz, Phys. Rev. Lett. **33**, 893 (1974).
[37] P. D. Gujrati, Phys. Rev. Lett. **74**, 809 (1995).
[38] R. J. Baxter, *Exactly Solved Models in Statistical Mechanics* (Academic Press, London, 1982).
[39] B. Bollobás, *Random Graphs* (Cambridge University Press, Cambridge, 2001) p. 53.
[40] E. DiMarzio, J. Chem. Phys. **35**, 658 (1961).
[41] J. F. Stilck and M. J. de Oliveira, Phys. Rev. A **42**, 5955 (1990).
[42] E. Botelho and J. F. Stilck, Phys. Rev. E **48**, 723 (1993).
[43] W. Selke, Phys. Rep. **170**, 213 (1988).